High-Order Cardiomyopathy Human Heart Model and Mesh Generation

Fariba Mohammadi[1,4], Suzanne M Shontz[2,3,4], Cristian A Linte[5,6]

[1] Department of Mechanical Engineering, [2] Department of Electrical Engineering and Computer Science, [3] Bioengineering Program, [4] Information and Telecommunication Technology Center, University of Kansas, Lawrence, KS, USA
[5] Chester F Carlson Center for Imaging Science, [6] Department of Biomedical Engineering, Rochester Institute of Technology, Rochester, NY, USA

Abstract

Faithful, accurate, and successful cardiac biomechanics and electrophysiological simulations require patient-specific geometric models of the heart. Since the cardiac geometry consists of highly-curved boundaries, the use of high-order meshes with curved elements would ensure that the various curves and features present in the cardiac geometry are well-captured and preserved in the corresponding mesh. Most other existing mesh generation techniques require computer-aided design files to represent the geometric boundary, which are often not available for biomedical applications. Unlike such methods, our technique takes a high-order surface mesh, generated from patient medical images, as input and generates a high-order volume mesh directly from the curved surface mesh. In this paper, we use our direct high-order curvilinear tetrahedral mesh generation method [1] to generate several second-order cardiac meshes. Our meshes include the left ventricle myocardia of a healthy heart and hearts with dilated and hypertrophic cardiomyopathy. We show that our high-order cardiac meshes do not contain inverted elements and are of sufficiently high quality for use in cardiac finite element simulations.

1. Introduction

Patient-specific geometric models of the heart are necessary in ensuring accurate and successful cardiac biomechanics and electrophysiological simulations. These simulations play a vital role in understanding normal cardiac function, as well as abnormal behavior due to various cardiovascular diseases. Such simulations can be performed using high-order partial differential equation solvers, such as finite element methods. To represent the highly-curved boundaries of the cardiac geometry, these solvers must be paired with high-order meshes consisting of curved elements. Moreover, computational modeling and simulation of the cardiac biomechanics would greatly benefit from the use of high-order meshes, yielding more accurate results with fewer mesh elements compared to its low-order counterpart. Thus, robust and high-quality, high-order meshes are an essential part of accurate and efficient cardiac simulations.

Biomedical meshing, specifically cardiac meshing, has attracted significant interest of many in recent years. Various mesh generation schemes have been developed and used by research groups to generate cardiovascular meshes [2–5]. Cardiac modeling and simulations of such meshes have been employed to understand the electrophysiology [3, 6] and mechanical deformation [6] of the heart. Also, researchers have studied cardiac flow simulations [7] and different cardiovascular conditions and diseases [3, 8] with the help of cardiac modeling and meshing. Most cardiovascular mesh generation strategies either generate low-order [2, 6] or coarse high-order meshes [4]. Cardiac meshes generated in [2, 6] are low-order meshes with a large number of mesh elements. In the absence of curved high-order meshes, such overrefined linear meshes are used to capture the curves present in the heart. However, such a large number of mesh elements results in a high computational cost. In [4], a high-order mesh generation scheme was used to generate cubic Hermite and cubic Lagrange cardiac ventricular meshes. These meshes are fairly coarse with 1, 12, and 6 and 2, 9, and 8 elements in the radial, circumferential, and longitudinal directions, respectively. In [5], another high-order mesh generation technique was employed to generate cubic Hermite meshes. This method involved a manual vertex placement strategy. Using an approach known as the immersed boundary method [9], the structural response of the human heart associated with blood flow was studied. In this method, the mesh is not required to conform to the complex geometrical structure of the heart. In contrast, using our method [1], we generate quadratic tetrahedral cardiovascular meshes where the mesh is fine enough to properly capture the

boundary representation and does not involve manual intervention. The novelty of our work lies in our method's ability to generate high-order meshes directly from curved boundaries. We use our method to generate meshes of various cardiovascular geometries where patient-specific models are obtained from medical images.

In this paper, we will use our high-order tetrahedral mesh generation technique [1] to obtain several second-order curvilinear meshes of various cardiomyopathies along with a healthy heart myocardium.

2.   Method

In earlier work [1, 10], we developed a direct method of high-order mesh generation using an advancing front approach [11].

2.1.   Initial Front Setup and Search for Candidate Vertices

We start with a high-order triangular surface mesh obtained from magnetic resonance images (MRI) images, and use it as the initial boundary representation. Each triangular face of the surface mesh is considered to be a member of the initial active front. Next, we calculate the area of each triangular element and average the areas of all the curved triangular elements. We use this average area to calculate a reference height h of a tetrahedron. Once the reference height is calculated, we select the first triangular face from the active front and insert a vertex at distance h from the centroid of that element in the inward normal direction. Next, we search for other suitable candidate vertices within a specific radius, $r = \alpha h$, as shown in Fig. 1. Here, α is a user-defined constant value that can be varied according to the size of the geometry and mesh.
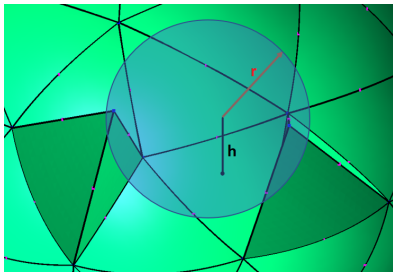

Figure 1. Candidate vertex search within radius r.

2.2.   Validity Check, Quality Tests, and Final Tetrahedral Element Generation

For each candidate tetrahedron obtained from the vertex search, we perform several validity checks and quality metric calculations to ensure we generate the best possible tetrahedron from among the available candidate vertices. The candidate tetrahedron that passes all validity and quality checks is selected as the final tetrahedron for that surface triangular face. If there is no suitable candidate element due to the possibility of colliding fronts from different directions, we perform local remeshing around the selected triangular face to obtain a valid tetrahedral element. In this process, we remove the tetrahedra that are near the selected surface triangle and remesh that region. Once we have generated a valid tetrahedron, we insert the high-order nodes in the element and perform mesh optimization [12]. The mesh optimization step utilizes the high-order degrees of freedom available in each element and further improves the quality of the mesh.

3.   Results

Our method is designed to generate meshes for various biomedical applications where no CAD file is available. In this section, we will show meshes of a healthy heart and also of different cardiomyopathies generated using our method. We use scaled Jacobian and equiangular skewness to assess the quality of our meshes.

For our examples, the geometric model of the left ventricle (LV) myocardium was obtained from cine cardiac magnetic resonance (MR) images using the Automated Cardiac Diagnosis Challenge (ACDC) dataset [13]. To generate the low-order surface mesh, the Lewiner marching cubes algorithm [14] was used, followed by mesh simplification in MeshLab [15]. After obtaining the low-order surface meshes, we use Gmsh [16] to introduce the high-order nodes onto the low-order surface mesh. Finally we used meshCurve [17] to curve the second-order surface mesh from the enriched linear surface mesh.

For our first example, we generate a second-order tetrahedral mesh of the left ventricle myocardium of a normal human heart. Figures 2(a,b,c) show the top, side, and cut plane view of the myocardium. The runtime statistics and mesh quality information are shown in Fig. 2(d).

For our second example, we generate a second-order mesh of the left ventricle of a human heart with dilated cardiomyopathy (DCM). With DCM, heart chambers become stretched, thin, and weakened. As a result, the heart cannot pump enough blood to the rest of the body. Figures 3(a,b,c) show the top, side, and cut plane view of the myocardium. The runtime statistics and mesh quality information are shown in Fig. 3(d).

Finally, we generated a second-order teterahedral mesh of the left ventricle of a human heart with hypertrophic cardiomyopathy (HCM). With HCM, heart muscle becomes abnormally thick (hypertrophied). The top, side, and cut plane view of the tetrahedral meshes of the myocardium with HCM are shown in Fig. 4(a,b,c). The runtime statis-
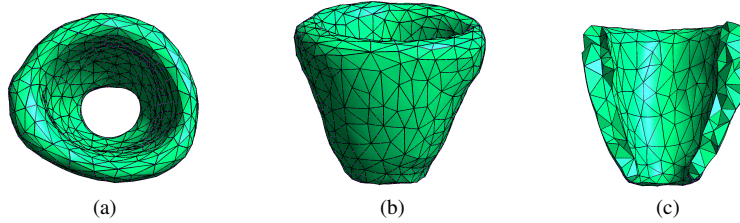
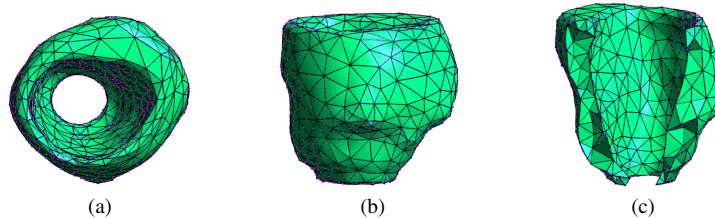| No. of Elements | Runtime (s) | | Scaled Jacobian | | | Equiangular skewness | | | |
			Initial	Final		Initial		Final	
	Mesh generation	Mesh optimization	min	min	max	min	max	min	max
3022	3283	0.203	0.123	1.000	0.156	1.000	0.041	0.895	0.013	0.883

(d)

Figure 2. Second-order curvilinear tetrahedral mesh of the LV myocardium of a normal human heart: (a) top view; (b) side view; (c) cross section, and (d) algorithm runtime statistics and mesh quality metrics.
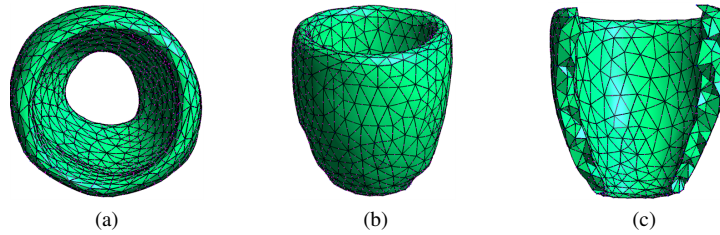
No. of Elements	Runtime (s)		Scaled Jacobian			Equiangular skewness			
			Initial	Final		Initial		Final	
	Mesh generation	Mesh optimization	min	min	max	min	max	min	max
5340	6712	0.219	0.126	1.000	0.169	1.000	0.023	0.879	0.020	0.875

(d)

Figure 3. Second-order curvilinear tetrahedral mesh of the LV myocardium with DCM: (a) top view; (b) side view; (c) cross section, and (d) algorithm runtime statistics and mesh quality metrics.

No. of Elements	Runtime (s)		Scaled Jacobian			Equiangular skewness			
			Initial	Final		Initial		Final	
	Mesh generation	Mesh optimization	min	min	max	min	max	min	max
3839	4672	0.103	0.106	1.000	0.110	1.000	0.036	0.919	0.029	0.897

(d)

Figure 4. Second-order curvilinear tetrahedral mesh of the LV myocardium with HCM: (a) top view; (b) side view; (c) cross section, and (d) algorithm runtime statistics and mesh quality metrics.

tics and mesh quality information are shown in Fig. 4(d).

4. Conclusion

In this paper, we used cardiac boundary representations obtained from MRI to generate several second-order tetrahedral meshes of the cardiac geometry. We generated meshes of three different LV myocardia. Our examples include both a healthy human heart as well as two hearts with cardiomyopathies. Cardiac simulations using these meshes would be very helpful in providing better insight on these conditions to medical doctors, and aid in understanding the effects of various cardiomyopathies on cardiac function. The meshes generated using our method are of high quality and can be used in cardiac simulations. However, the quality of our meshes are also dependent on that of the input surface meshes. Our future work will include dynamic cardiac mesh generation, as well as extending our method to generate cardiac meshes that include additional features, such as the cardiac fiber architecture.

Acknowledgments

References

[1] Mohammadi F, Shontz SM. A direct method of generating quadratic curvilinear tetrahedral meshes using an advancing front approach. Proceedings of the 29th International Meshing Roundtable, to appear, 2021.

[2] Zhang Y, Bajaj C. Finite element meshing for cardiac analysis. ICES Technical Report 04-26, The University of Texas at Austin, 2004.

[3] Lamecker H, Mansi T, Relan J, Billet F, Sermesant M, Ayache N, Delingette H. Adaptive tetrahedral meshing for personalized cardiac simulations. In CI2BM09-MICCAI Workshop on Cardiovascular Interventional Imaging and Biophysical Modelling. 2009; 149–158.

[4] Lamata P, Sinclair M, Kerfoot E, Lee A, Crozier A, Blazevic B, Land S, Lewandowski AJ, Barber D, Niederer S, et al. An automatic service for the personalization of ventricular cardiac meshes. Journal of The Royal Society Interface 2014;11(91):20131023.

[5] Gonzales MJ, Sturgeon G, Krishnamurthy A, Hake J, Jonas R, Stark P, Rappel WJ, Narayan SM, Zhang Y, Segars WP, et al. A three-dimensional finite element model of human atrial anatomy: New methods for cubic Hermite meshes with extraordinary vertices. Medical Image Analysis 2013; 17(5):525–537.

[6] Baillargeon B, Rebelo N, Fox DD, Taylor RL, Kuhl E. The living heart project: A robust and integrative simulator for human heart function. European Journal of Mechanics A Solids 2014;48:38–47.

[7] Sahni O, Jansen KE, Taylor CA, Shephard MS. Automated adaptive cardiovascular flow simulations. Engineering with Computers 2009;25(1):25–36.

[8] Einstein DR, Del Pin F, Jiao X, Kuprat AP, Carson JP, Kunzelman KS, Cochran RP, Guccione JM, Ratcliffe MB. Fluid–structure interactions of the mitral valve and left heart: Comprehensive strategies, past, present and future. International Journal for Numerical Methods in Biomedical Engineering 2010;26(3-4):348–380.

[9] Griffith BE, Hornung RD, McQueen DM, Peskin CS. An adaptive, formally second order accurate version of the immersed boundary method. Journal of Computational Physics 2007;223(1):10–49.

[10] Mohammadi F, Dangi S, Shontz SM, Linte CA. A direct high-order curvilinear triangular mesh generation method using an advancing front technique. In International Conference on Computational Science, volume 12138 of Lecture Notes in Computer Science. Springer, 2020; 72–85.

[11] Löhner R, Parikh P. Generation of three-dimensional unstructured grids by the advancing-front method. International Journal for Numerical Methods in Fluids 1988; 8(10):1135–1149.

[12] Geuzaine C, Johnen A, Lambrechts J, Remacle JF, Toulorge T. The generation of valid curvilinear meshes. In IDI-HOM: Industrialization of High-Order Methods - A Top-Down Approach. Springer, 2015; 15–39.

[13] Upendra RR, Wentz BJ, Simon R, Shontz SM, Linte CA. CNN-based cardiac motion extraction to generate deformable geometric left ventricle myocardial models from cine MRI. In International Conference on Functional Imaging and Modeling of the Heart. Springer, 2021; 253–263.

[14] Lewiner T, Lopes H, Vieira AW, Tavares G. Efficient implementation of marching cubes' cases with topological guarantees. Journal of Graphics Tools 2003;8(2):1–15.

[15] Cignoni P, Callieri M, Corsini M, Dellepiane M, Ganovelli F, Ranzuglia G. MeshLab: an Open-Source Mesh Processing Tool. In Scarano V, Chiara RD, Erra U (eds.), Eurographics Italian Chapter Conference. The Eurographics Association. ISBN 978-3-905673-68-5, 2008; .

[16] Geuzaine C, Remacle JF. Gmsh: A 3-D finite element mesh generator with built-in pre-and post-processing facilities. International Journal for Numerical Methods in Engineering 2009;79(11):1309–1331.

[17] Ims J, Duan Z, Wang ZJ. meshcurve: An automated low-order to high-order mesh generator. In Proceedings of The 22nd AIAA Computational Fluid Dynamics Conference. 2015; 2293.

Address for correspondence:

Fariba Mohammadi
University of Kansas, 1530 West 15th Street, 3138 Learned Hall, Lawrence, KS 66045
fariba_m@ku.edu